ACS central science

Research Article

http://pubs.acs.org/journal/acscii

Rechargeable Sodium All-Solid-State Battery

Weidong Zhou, Yutao Li,* Sen Xin, and John B. Goodenough*

Materials Research Program and the Texas Materials Institute, The University of Texas at Austin, Austin, Texas 78712, United States

Supporting Information

ABSTRACT: A reversible plating/stripping of a dendrite-free metallic-sodium anode with a reduced anode/ceramic interfacial resistance is created by a thin interfacial interlayer formed *in situ* or by the introduction of a dry polymer film. Wetting of the sodium on the interfacial interlayer suppresses dendrite formation and growth at different discharge/charge C-rates. All-solid-state batteries were obtained with a high cycling stability and Coulombic efficiency at 65 °C.

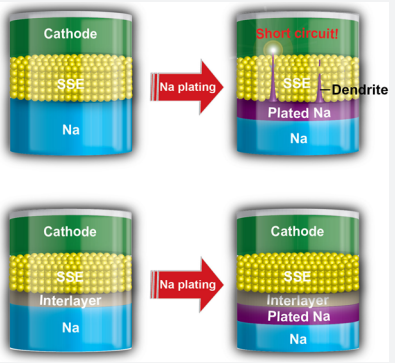

INTRODUCTION

Rechargeable Na-ion batteries have a cost advantage for large-scale stationary storage of electric power generated by solar and/or wind power owing to the widespread availability of Na in the oceans.[1−5] To meet the requirements of high energy density, safety, and long cycle life, it is necessary to replace the hard-carbon anode of the Na-ion battery by a metallic-sodium anode that can be plated/stripped reversibly without dendrites from a solid electrolyte; the electrolyte should have an energy gap large enough that the electrolyte is not reduced beyond a thin surface layer that allows a low impedance for Na^+ transfer between the anode and electrolyte.[6−13] The solid electrolyte needs to be wetted by metallic sodium and to have a Na^+ conductivity $\sigma_{Na} \gtrsim 10^{-4}$ S cm^{-1} at the operating temperature, which would preferably be room temperature. To date, ceramic Na^+ electrolytes, Na super ionic conductor (NASICON) with the $Na_{1+3x}Zr_2(P_{1-x}Si_xO_4)_3$ structure, have reached a $\sigma_{Na} \simeq 10^{-3}$ S cm^{-1} at $T \gtrsim 65$ °C, but they have been plagued by a large interfacial impedance; and anode dendrite formation is followed by rapid penetration of grain boundaries (Figure 1a).[14,15] Moreover, the volume changes of the electrodes over a charge/discharge cycle have prevented retention over many cycles of a solid−solid electrode−electrolyte interface. The interface problems of an alkali-metal/ceramic contact over many charge−discharge cycles may be largely overcome by the existence of a stable interface interstitial interlayer that is wetted by the anode and is a conductor of the working ion.[16,17] This observation has motivated an exploration of two avenues for creating the interface interstitial layer for a rechargeable sodium anode with a NASICON ceramic,[18,19] $Na_{1+3x}Zr_2(P_{1-x}Si_xO_4)_3$ with $x \approx 2/3$: (1) *in situ* formation of a Na^+-conductive thin layer and (2) introduction of a dry Na^+-conductive thin polymer layer. As illustrated in Figure 1b, the grain boundaries of the ceramic do not contact directly the sodium anode with an interfacial interlayer that undergoes homogeneous wetting by the sodium anode.

RESULTS AND DISCUSSION

The ceramic pellets of $Na_3Zr_2(PO_4)(SiO_4)_2$ were prepared by spark-plasma sintering (SPS) as previously reported;[18,20] the XRD spectra of the pellets verified single-phase formation of the NASICON structure. Scanning electron microscopy (SEM) images of the NASICON pellets are shown in Figure S1; numerous nanospheres of the ceramic were homogeneously melted and bonded together to form a solid substrate; no evidence of cracks or interparticle pores was observed in the thin pellets.

Wetting with an Interlayer Formed *in Situ*. NASICON $Na_3Zr_2Si_2PO_{12}$ gradually reacts with molten sodium at temperatures over 300 °C.[21,22] However, a $Na_3Zr_2Si_2PO_{12}$ membrane is quite stable toward sodium metal at lower temperatures. After heating of the sodium metal on the surface of the NASICON pellet at 175 °C for 5 h, no obvious change can be observed (Figure 2a). At 175 °C, liquid sodium metal stays on the NASICON pellet surface as a bead, indicating that the sodium metal has a stronger bonding with itself than with the surface of a NASICON pellet. On the other hand, a black layer on the surface of NASICON was formed when the pellet and sodium metal were heated at 380 °C for 30 min (Figure 2b and Figure S2). Moreover, the sodium metal spread out over the surface of the NASICON pellet, indicating that the black interlayer is wetted by the sodium metal.

X-ray photoelectron spectroscopy (XPS) of the 380 °C heat-treated NASICON (H-NASICON) pellets in the presence of sodium metal exhibited an obvious shift to lower energy of the elements of Zr, Si, and P (Figures 2c−2e). The Zr^{4+} $3d_{3/2}$ and $3d_{5/2}$ peaks at 185.02 and 182.63 eV in $Na_3Zr_2Si_2PO_{12}$ shifted, respectively, to 184.08 and 181.67 eV on the H-NASICON. The Si 2p peaks shifted from 102.02 to 101.00 eV. The P 2p peak at

Received: October 28, 2016
Published: January 3, 2017

DOI: 10.1021/acscentsci.6b00321
ACS Cent. Sci. 2017, 3, 52−57

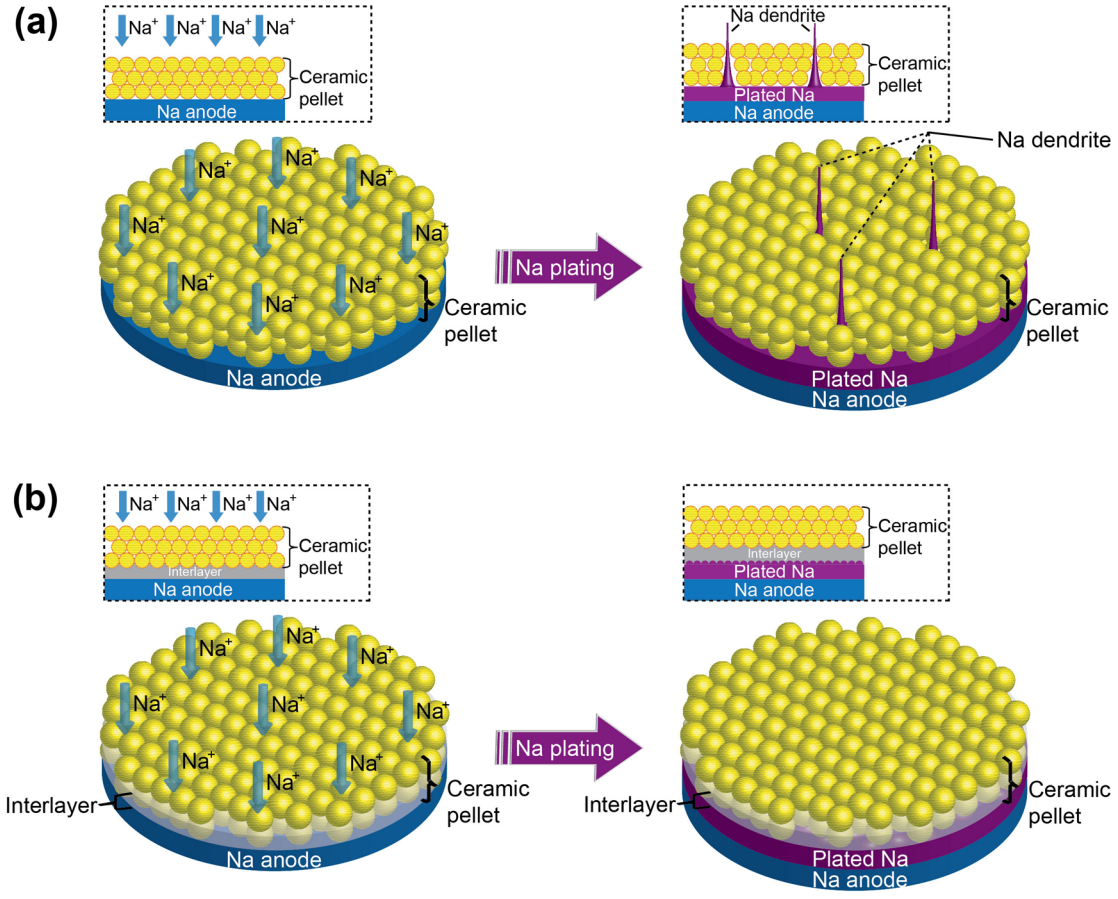

Figure 1. Contact model of ceramic pellet solid electrolyte and sodium metal with (a) a poor wetting ability ceramic pellet and (b) a good wetting ability artificial interlayer during the plating of sodium.

133.3 eV shifted to 132.4 eV. The only exception was the oxygen; no significant O^{2-} 2p binding energy difference was detected in H-NASICON (Figure S3). These XPS peak shifts on P, Si, and Zr indicate that the surface of the H-NASICON was partially reduced by the sodium metal to form an *in situ* interlayer. The XRD pattern of the H-NASICON with the black layer did not show extra signals compared with the $Na_3Zr_2Si_2PO_{12}$ (red line in Figure 2f). To get more information on the black species, the NASICON powder was treated with sodium metal at 380 °C for 2 h and XRD was then taken. Much weaker NASICON diffraction signals were detected without an additional signal of a new phase although all the powder became black-brown (blue line in Figure 2f), indicating that the black species is amorphous. In addition, we found that the black-brown powder returned white and the NASICON phase was recovered by heating the H-NASICON samples at 950 °C for 2 h in air (wine line in Figure 2f). These phenomena verified that the H-NASICON was partially reduced by sodium metal at high temperature.

In order to investigate the electrochemical performance of the NASICON pellet as a solid electrolyte for Na-ion batteries, typical 2032 coin cells were assembled in a glovebox. The impedance spectra of the Na/NASICON/Na and Na/H-NASICON/Na cells were first studied and are presented in Figure 3a; compared with the spectrum of the Na/NASICON/Na, the resistance of the Na/H-NASICON/Na is obviously lowered from 4000 to 400 ohm cm^{-2}, which can be attributed to the better wetting and adhesion across the Na/H-NASICON interface.

The electrochemical stability window of the solid electrolyte was then examined in a cell of Na/H-NASICON/gold-foil. The positive scan of the cyclic voltammetry (CV) curves in Figure 3b shows that the electrolyte did not experience obvious oxidation until 5 V, which indicates that the electrolyte membrane could be stable under 5 V. This electrochemical working window is capable of satisfying the requirement of most of the sodium-ion cathodes since they are generally operated at lower than 4.2 V. On the negative scan, the H-NASICON electrolytes experienced a symmetric lithium plating−stripping curve at −0.5−0.5 V; the sodium plating−stripping curves were similar, indicating a good electrochemical efficiency.

The electrochemical stability and whether anode dendrites form at the electrolyte interface were then evaluated in sodium/sodium symmetric cells by periodically charging for 1 h and discharging for 1 h. Figure 3c and S4 show the time-dependent voltage profiles for Na/Na symmetric cells with the H-NASICON and NASICON pellet electrolyte under a constant current density of 0.15 mA cm^{-2} and then increased to 0.25 mA cm^{-2}. As shown in Figure 3c, the cell with the H-NASICON delivered stable sodium plating−stripping cycles for up to 550 h; the voltage did not show any significant increase/decrease, indicating that either the dendrite growth was blocked or dendrite formation was suppressed in the Na/H-NASICON interface during long-term cycling. On the contrary, the Na/NASICON/Na symmetric cells short-circuited in only 1 h under a current density of 0.15 mA cm^{-2} owing to a rapid dendrite formation and penetration of the grain boundaries (Figure S4), similar to other lithium ceramic electrolytes such as the garnet $Li_7La_3Zr_2O_{12}$ (LLZO).[14,15] Interestingly, we found that the ceramic pellets synthesized by SPS showed an even faster short-circuit in the Na/Na symmetric

DOI: 10.1021/acscentsci.6b00321
ACS Cent. Sci. 2017, 3, 52−57

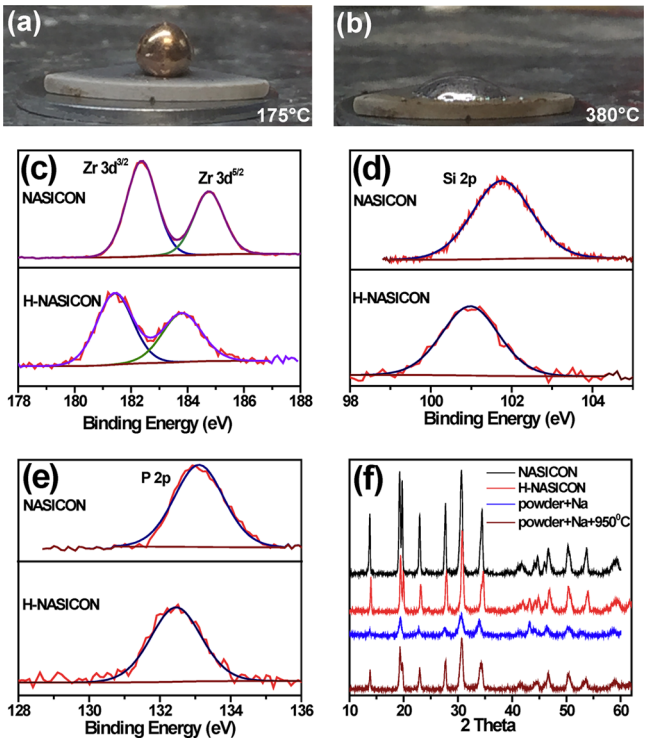

Figure 2. Optical photos of sodium metal on a NASICON pellet (a) at 175 °C and (b) at 380 °C. XPS data of (c) Zr, (d) Si, and (e) P before and after reaction with Na metal at 380 °C for 0.5 h. (f) The XRD spectra of the $Na_3Zr_2Si_2PO_{12}$ NASICON (black line), H-NASICON (red line), and heat treated NASICON powder with Na metal for 2 h (blue line) and then heated at 950 °C for 2 h in air (wine line).

cells than the symmetric cells with pellets synthesized by a conventional sintering process in a regular heating oven (Figures S5 and S6), which can be attributed to the formation of narrower grain boundaries in pellets synthesized by SPS. Since the sodium tends to plate on the grain boundaries where the electric field is enhanced locally during charge, the narrower grain boundaries only allow the growth of thinner dendrites and therefore lead to a more rapid dendrite penetration. Figures 3d and 3e give the SEM images of sodium metal after cycling in a Na/H-NASICON/Na cell; uniform sodium plating can be observed without obvious sodium dendrite formation although the sodium-metal surface showed some cracks after cycling owing to the volume expansion during plating.[23,24] On the contrary, uneven sodium plating and obvious dendrite growth were clearly observed on the surface of the sodium metal after cycling in a Na/NASICON/Na cell (Figure S7). These phenomena indicate that the interlayer formed *in situ* between sodium metal and ceramic pellets not only effectively lowers the interfacial resistance but also successfully suppresses dendrite formation owing to a better wetting of the interlayer; wetting by the sodium metal gives a more uniform sodium flux across the interface.

The H-NASICON pellet electrolyte was then tested in a $NaTi_2(PO_4)_3$/H-NASICON/Na all-solid-state cell since $NaTi_2(PO_4)_3$ has been shown to have a stable capacity during long-term sodiation−desodiation in both liqiud[25] and polymer[26] electrolytes. The $NaTi_2(PO_4)_3$ cathode membranes were prepared with cross-linked poly(ethylene glycol) methyl ether acrylate (CPMEA) as a Na^+-conducting binder and carbon black as the electron conductor. The CPMEA consists of an electrochemically inert polyacrylate framework and soft oligo-ethylene oxide pendants, which realizes an acceptable solid-state ionic conductivity through a swing of the pendant groups in the polymer framework.[16] The ionic conductivity of the CPMEA shows a gradual increase with increasing temperature, reaching 0.7×10^{-4} S cm^{-1} at 65 °C owing to the increasing movement of the oligo-ethylene oxide pendants in the polymer network (Figure S8). Figures 4a and 4b show, respectively, the charge/discharge voltage profiles and the cycling performance of a cell at different rates at 65 °C. The one flat plateau at 2.1 V and a capacity of around 110 mAh g^{-1} at 0.2 C are the characteristic behavior of $NaTi_2(PO_4)_3$ electrodes, indicating that the H-NASICON can function effectively as a solid electrolyte in an all-solid-state sodium battery. In long cycling, the discharge capacity is generally around 110 mAh g^{-1} at 0.2 C rate during the first 25 cycles and is slightly higher than 75 mAh g^{-1} at 1 C during the following 35 cycles. When the C rate was switched to 0.5 C, a capacity of 94 mAh g^{-1} could be recovered. It is remarkable that the Coulombic efficiency is always kept at 99.8 ± 0.2% at all three C-rates after the initial formation cycles, indicating high sodium plating/stripping efficiency and good electrochemical stability across the Na/H-NASICON interface. More importantly, this long cycling stability also verifies the good capability of dendrite suppression at a Na/H-NASICON interface since the cell should have short-circuited if a dendrite had penetrated across the H-NASICON pellet.

Wetting with a Dry Polymer Interlayer. We have reported a sandwich electrolyte of polymer/ceramic-pellet/polymer to plate a dendrite-free lithium anode.[16] The polymer used in our previous report was CPMEA, the same polymer used in this study. The polymer interlayer between lithium and ceramic was wetted well by the lithium metal, which homogenized the Li-ion flux across the interface. An all-solid-state Li/CPMEA/ceramic/CPMEA/$LiFePO_4$ battery with a notably high Coulombic efficiency of 99.8%−100% over 600 cycles was obtained. To investigate further whether this sandwich electrolyte is effective in a sodium-based all-solid-state battery, a CPMEA/NASICON/CPMEA sandwich electrolyte was fabricated with the previous method. Figure 5a shows the impedance spectra of a Na/CPMEA/NASICON/CPMEA/Na cell, which is also obviously lower than that of the Na/NASICON/Na, indicating that the polymer inerlayer improves the ionic conductivity across the solid Na/NASICON interface. The resistance is a little higher than that of the Na/H-NASICON/Na, which can be attributed to the internal resistance of the polymer layer and a new interfacial impedance across CPMEA/NASICON interfaces. The symmetric cell of Na/CPMEA/NASICON/CPMEA/Na was then tested to evaluated the polymer stability and dendrite suppression performance on repeated sodium plating and stripping, as is shown in Figure 5b. The cell gave a stable voltage profile for up to 380 h under a constant current density of 0.20 mA cm^{-2} after an obvious voltage decrease during the initial 2 h owing to an interfacial wetting process, indicating that the sodium dendrite was also suppressed by the polymer interlayer and the Na/CPMEA/NASICON interface is stable during repeated sodium plating−stripping cycles.

The stability of the solid sandwich electrolyte was then further evaluated in $NaTi_2(PO_4)_3$/Na cells with a CPMEA/NASICON double layer electrolyte since the cathode films were prepared with the polymer electrolyte as the binder. As shown in Figures 5c and 5d, a stable capacity of around 102 mAh g^{-1} was obtained for 70 cycles at 0.2 C and 65 °C; the Coulombic efficiency remained at 99.7 ± 0.3% during this cycling, indicating good stability of the Na/CPMEA/NASICON interfaces and capability of dendrite suppression during the charge/discharge

DOI: 10.1021/acscentsci.6b00321
ACS Cent. Sci. 2017, 3, 52−57

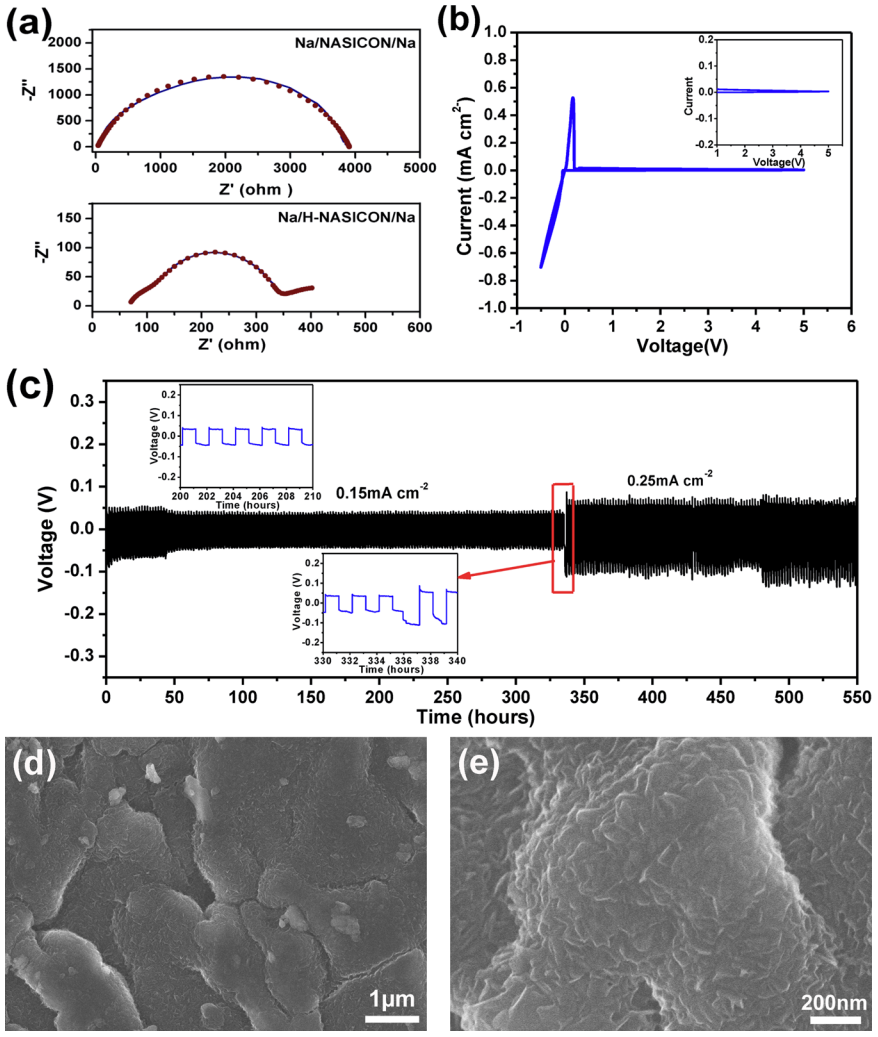

Figure 3. (a) The impedance plots of Na/NASICON/Na and Na/H-NASICON/Na symmetric cell at 65 °C. (b) CV curve of a Na/H-NASICON/gold-foil at a scanning rate of 0.5 mV s^{-1}. (c) Cycling stability test of the Na/H-NASICON/Na symmetric cells at 65 °C. (d, e) Surface SEM images of sodium metal anode after cycling in the Na/H-NASICON/Na cell.

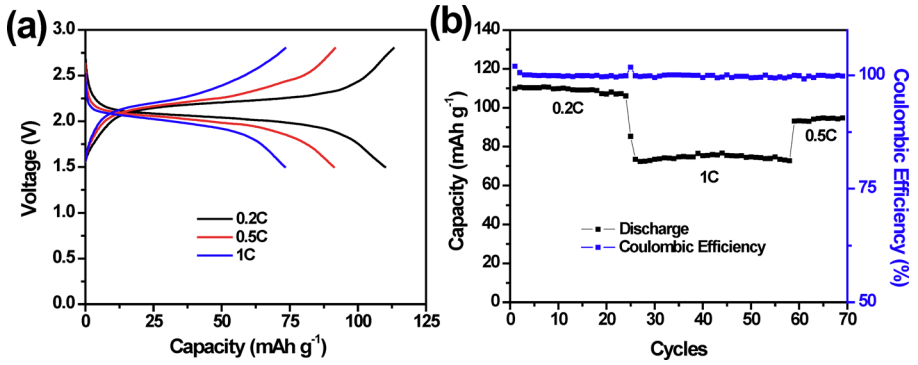

Figure 4. (a) Charge and discharge voltage profiles and (b) cycling performance of $NaTi_2(PO_4)_3$/Na cell with a H-NASICON pellet electrolyte at different C-rates and 65 °C.

process, which are comparable to the Na/H-NASICON interface.

A large interface resistance and severe dendrite formation across an alkali-metal/ceramic interface are two critical factors that have restricted the application of ceramic electrolytes in all-solid-state batteries. If the untreated NASICON pellets are employed, the sodium does not wet the ceramic electrolyte and, therefore, uniform Na^+ flux across the interface is not established. As a result, the Na^+ ions plate preferentially on the grain boundaries where the Na^+ flux is locally enhanced under an electronic field and dendrites nucleate and grow there during a charge. Since the grain boundaries are usually interconnected, the dendrites can penetrate the ceramic in a short time.[14,15] With an interface interlayer, a homogeneous ceramic/interlayer/sodium interface gives a more uniform Na-flux across the interface since the sodium metal wets better the interlayer than the ceramic.

DOI: 10.1021/acscentsci.6b00321
ACS Cent. Sci. 2017, 3, 52−57

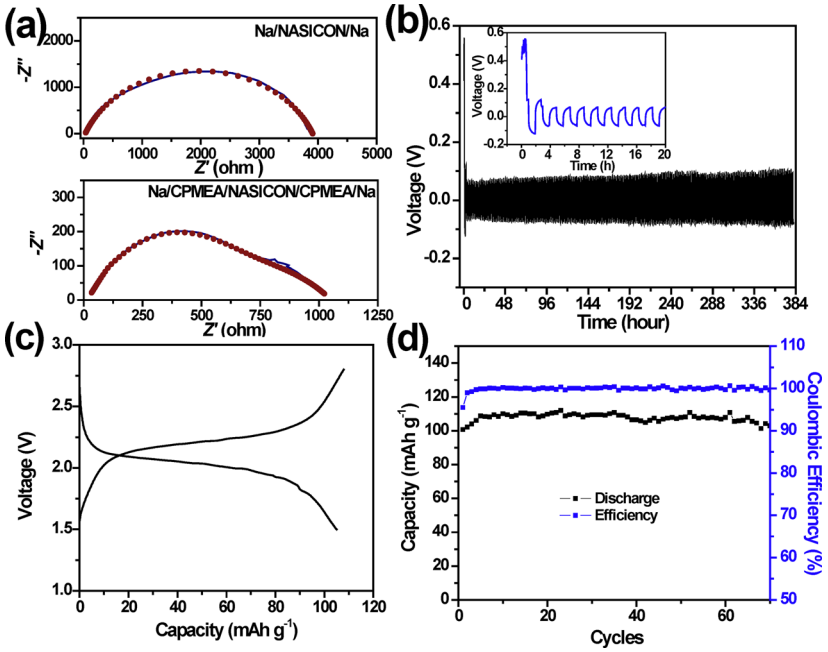

Figure 5. (a) The impedance spectra of a Na/Na cell with a CPMEA/NASICON/CPMEA electrolyte. (b) Voltage profiles of a symmetric Na/Na cell with a CPMEA/NASICON/CPMEA sandwich electroyte cycled at 65 °C. (c) Charge−discharge voltage profiles and (d) cycling performance of a $NaTi_2(PO_4)_3$/Na cell with CPMEA/NASICON as the electrolyte at 0.2 C and 65 °C.

Moreover, the anode−interlayer bonding restricts expansion/contraction of the anode during plating/stripping to be perpendicular to the interface to give the interface a long cycle life.

We have presented here two strategies to fabricate an interface interlayer between a Na metal and a ceramic NASICON electrolyte: heat treated NASICON in the presence of Na metal and a polymer/NASICON/polymer sandwich. Better wetting of the electrolyte by the sodium anode gives a uniform Na^+ flux across the interface, which not only dramatically lowers the interface resistance but also successfully suppresses unwanted dendrite formation. A good cycling performance and high efficiency of all-solid-state sodium cells were demonstrated with two types of strategies for good electrochemical stability and high sodium plating/stripping efficiency across a Na/ceramic interface.

■ ASSOCIATED CONTENT

Supporting Information

The Supporting Information is available free of charge on the ACS Publications website at DOI: 10.1021/acscentsci.6b00321.

Detailed characterization and electrochemical performance (PDF)

■ AUTHOR INFORMATION

Corresponding Authors

*E-mail: lytthu@gmail.com.

*E-mail: jgoodenough@mail.utexas.edu.

ORCID

Sen Xin: 0000-0002-0546-0626

John B. Goodenough: 0000-0001-9350-3034

Notes

The authors declare no competing financial interest.

■ ACKNOWLEDGMENTS

W.Z. was supported by the National Science Foundation, Grant No. CBET-1438007, and Y.L. by the U.S. Department of Materials Science and Engineering under Award No. DOE-SC0005397. S.X. participated in discussion and preparation of the manuscript; J.B.G. supervised the project.

■ REFERENCES

(1) Tarascon, J. M. Is lithium the new gold? *Nat. Chem.* **2010**, *2*, 510.

(2) Palomares, V.; Serras, P.; Villaluenga, I.; Hueso, K. B.; Carretero-Gonzalez, J.; Rojo, T. Na-ion batteries, recent advances and present challenges to become low cost energy storage systems. *Energy Environ. Sci.* **2012**, *5*, 5884−5901.

(3) Slater, M. D.; Kim, D.; Lee, E.; Johnson, C. S. Sodium-Ion batteries. *Adv. Funct. Mater.* **2013**, *23*, 947−958.

(4) Pan, H. L.; Hu, Y. S.; Chen, L. Q. Room-temperature stationary sodium-ion batteries for large-scale electric energy storage. *Energy Environ. Sci.* **2013**, *6*, 2338−2360.

(5) Kundu, D.; Talaie, E.; Duffort, V.; Nazar, L. F. The emerging chemistry of sodium ion batteries for electrochemical energy storage. *Angew. Chem., Int. Ed.* **2015**, *54*, 3431−3448.

(6) Tarascon, J. M.; Armand, M. Issues and challenges facing rechargeable lithium batteries. *Nature* **2001**, *414*, 359−367.

(7) Xu, K. Electrolytes and interphases in Li-Ion batteries and beyond. *Chem. Rev.* **2014**, *114*, 11503−11618.

(8) Armand, M.; Tarascon, J. M. Building better batteries. *Nature* **2008**, *451*, 652−657.

(9) Croce, F.; Appetecchi, G. B.; Persi, L.; Scrosati, B. Nanocomposite polymer electrolytes for lithium batteries. *Nature* **1998**, *394*, 456−458.

(10) Liu, W.; Liu, N.; Sun, J.; Hsu, P.-C.; Li, Y.; Lee, H.-W.; Cui, Y. Ionic conductivity enhancement of polymer electrolytes with ceramic nanowire fillers. *Nano Lett.* **2015**, *15*, 2740−2745.

(11) Cao, C.; Li, Z.-B.; Wang, X.-L.; Zhao, X.-B.; Han, W.-Q. Recent advances in inorganic solid electrolytes for lithium batteries. *Front. Energy Res.* **2014**, *2*, 25.

(12) Quartarone, E.; Mustarelli, P. Electrolytes for solid-state lithium rechargeable batteries: recent advances and perspectives. *Chem. Soc. Rev.* **2011**, *40*, 2525−2540.

(13) Goodenough, J. B.; Singh, P. Review−solid electrolytes in rechargeable electrochemical cells. *J. Electrochem. Soc.* **2015**, *162*, A2387−A2392.

DOI: 10.1021/acscentsci.6b00321
ACS Cent. Sci. 2017, 3, 52−57

(14) Sudo, R.; Nakata, Y.; Ishiguro, K.; Matsui, M.; Hirano, A.; Takeda, Y.; Yamamoto, O.; Imanishi, N. Interface behavior between garnet-type lithium-conducting solid electrolyte and lithium metal. *Solid State Ionics* **2014**, *262*, 151−154.
(15) Ren, Y.; Shen, Y.; Lin, Y.; Nan, C.-W. Direct observation of lithium dendrites inside garnet-type lithium-ion solid electrolyte. *Electrochem. Commun.* **2015**, *57*, 27−30.
(16) Zhou, W.; Wang, S.; Li, Y.; Xin, S.; Manthiram, A.; Goodenough, J. B. Plating a dendrite-free lithium anode with a polymer/ceramic/polymer sandwich electrolyte. *J. Am. Chem. Soc.* **2016**, *138*, 9385−9388.
(17) Hood, Z. D.; Wang, H.; Samuthira Pandian, A.; Keum, J. K.; Liang, C. Li_2OHCl crystalline electrolyte for stable metallic lithium anodes. *J. Am. Chem. Soc.* **2016**, *138*, 1768−1771.
(18) Goodenough, J. B.; Hong, H. Y-P.; Kafalas, J. A. Fast Na^+-ion transport in skeleton structures. *Mater. Res. Bull.* **1976**, *11*, 203−220.
(19) Kim, Y.; Kim, H.; Park, S.; Seo, I.; Kim, Y. Na ion-conducting ceramic as solid electrolyte for rechargeable seawater batteries. *Electrochim. Acta* **2016**, *191*, 1−7.
(20) Zhou, M.; Ahmad, A. Synthesis, processing and characterization of nasicon solid electrolytes for CO_2 sensing applications. *Sens. Actuators, B* **2007**, *122*, 419−426.
(21) Anantharamulu, N.; Koteswara Rao, K.; Rambabu, G.; Vijaya Kumar, B.; Radha, V.; Vithal, M. A wide-ranging review on Nasicon type materials. *J. Mater. Sci.* **2011**, *46*, 2821−2837.
(22) Kuriakose, A. K.; Wheat, T. A.; Ahmad, A.; DiRocco, J. Synthesis, sintering, and microstructure of nasicons. *J. Am. Ceram. Soc.* **1984**, *67*, 179−183.
(23) Ding, F.; Xu, W.; Graff, G. L.; Zhang, J.; Sushko, M. L.; Chen, X.; Shao, Y.; Engelhard, M. H.; Nie, Z.; Xiao, J.; Liu, X.; Sushko, P. V.; Liu, J.; Zhang, J. G. Dendrite-free lithium deposition via self-healing electrostatic shield mechanism. *J. Am. Chem. Soc.* **2013**, *135*, 4450−4456.
(24) Zhang, Y.; Qian, J.; Xu, W.; Russell, S. M.; Chen, X.; Nasybulin, E.; Bhattacharya, P.; Engelhard, M. H.; Mei, D.; Cao, R.; Ding, F.; Cresce, A. V.; Xu, K.; Zhang, J. G. Dendrite-free lithium deposition with self-aligned nanorod structure. *Nano Lett.* **2014**, *14*, 6889−6896.
(25) Park, S. I.; Gocheva, I.; Okada, S.; Yamaki, J. Electrochemical properties of $NaTi_2(PO_4)_3$ anode for rechargeable aqueous sodium-ion batteries. *J. Electrochem. Soc.* **2011**, *158*, A1067−A1070.
(26) Zhou, W.; Gao, H.; Goodenough, J. B. Low-Cost Hollow Mesoporous Polymer Spheres and All-Solid-State Lithium, Sodium Batteries. *Adv. Energy Mater.* **2016**, *6*, 1501802.

DOI: 10.1021/acscentsci.6b00321
ACS Cent. Sci. 2017, 3, 52−57